

Electronic Supplemental Information for

Noncovalent phosphorylation of graphene oxide with improved hole transport in high-efficiency polymer solar cells

Xiang Chen,^a Qing Liu,^a Mengmeng Zhang,^a Huanxin Ju,^b Junfa Zhu,^b Qiquan Qiao,^{c,*} Mingtai Wang,^d and Shangfeng Yang^{a,*}

^a Hefei National Laboratory for Physical Sciences at Microscale, Key Laboratory of Materials for Energy Conversion, Chinese Academy of Sciences, Department of Materials Science and Engineering, Synergetic Innovation Center of Quantum Information & Quantum Physics, University of Science and Technology of China, Hefei 230026, China
E-mail: sfyang@ustc.edu.cn

^b National Synchrotron Radiation Laboratory, University of Science and Technology of China, Hefei 230029, China

^c Center for Advanced Photovoltaics, Department of Electrical Engineering and Computer Science, South Dakota State University, Brookings, SD 57007, USA
E-mail: Qiquan.Qiao@sdstate.edu

^d Institute of Applied Technology, Hefei Institutes of Physical Science, Chinese Academy of Sciences, Hefei 230088, China

Contents

S1. Experimental Section.

S2. Mass spectrum of $(\text{CH}_3\text{O})_x\text{PO}(\text{OH})_{3-x}$.

S3. Effect of spin-coating speed of P_2O_5 solution on the performance of P-GO-based devices.

S4. Effect of the initial concentration of P_2O_5 dissolved in methanol solution on the performance of P-GO-based devices.

S5. Effect of spin-coating speed of GO dispersion on the performance of GO-based devices.

S6. Photovoltaic performance of P3HT:PC₆₁BM devices based on different HTLs.

S7. Transmittance spectra of ITO, ITO/PEDOT:PSS, ITO/GO and ITO/P-GO layers.

S8. Photovoltaic performance of PTB7-Th:PC₇₁BM devices based on different HTLs.

S9. Enhancement ratios of the photovoltaic parameters.

S10. Contact angles of water droplet on bare ITO, PEDOT:PSS, GO, and P-GO.

S11. Work functions of ITO, PEDOT:PSS, GO, and P-GO.

S12. High-resolution P2p XPS spectra of $(\text{CH}_3\text{O})_x\text{PO}(\text{OH})_{3-x}$ and $(\text{CH}_3\text{O})_x\text{PO}(\text{OH})_{3-x}/\text{GO}$.

S13. Raman spectra of GO and P-GO.

S14. Hole mobilities of the devices with different HTLs.

S1. Experimental Section

Materials.

Graphite powder was purchased from Aladdin. P_2O_5 , $K_2S_2O_8$, H_2O_2 and $KMnO_4$ were purchased from Sinopharm Chemical reagent Co. Ltd. Poly (3,4-ethylenedioxythiophene):polystyrene sulfonic acid (PEDOT:PSS, Clevios P AI4083) was purchased from SCM Industrial Chemical Co., Ltd. P3HT, PBDTTT-C, $PC_{61}BM$, $PC_{71}BM$ were bought from Luminescence Technology Corp., Solarmer Material Inc., Nichem Fine Technology Co., Ltd. and Solenne BV., respectively. Both PTB7 and PTB7-Th were bought from 1-Material. All chemicals were used as received without further purification.

Synthesis of GO.

A mixture of 0.60 g graphite powder, 1.00 g P_2O_5 , 4.80 mL concentrated H_2SO_4 , and 1.00 $K_2S_2O_8$ was stirred for 4.5 h in an oil bath at 80 °C and then was slowly added 200 mL water, followed by filtered and dried in vacuum. The solid was added into flask with 24 mL concentrated H_2SO_4 and stirred in an ice-water bath and then 3 g $KMnO_4$ was slowly added. The flask was transferred to oil bath at 35 °C for 2h, then diluted with 50 mL water and heated for 2 h at 35 °C continually. After cooled down, the mixture was slowly added into 140 mL deionized water and 4 mL H_2O_2 , followed by filtered and washed with diluted hydrochloric acid. The resultant solid was then dispersed in water by ultrasonication for 10 h and centrifugation at 5000 rpm for 10 min. After the supernatant was purified through dialysis and diluted with deionized water, 0.5 mg/mL aqueous GO solution was obtained.

Device Fabrication.

The ITO-coated glass substrate ($10 \Omega/\square$) was cleaned with detergent, deionized water, acetone and isopropanol for 15 min every time, and subsequently dried in an oven overnight at 60 °C. ITO was treated with UV light for 14 min, to prepare the device with P-GO as hole transport layer, 0.5 mg/mL aqueous GO dispersion was spin-coated onto ITO at 2000 rpm for 60 s and heated at 120°C for 30 min, followed by spin-coated 0.2 mg/mL P_2O_5 at 2000 rpm for 60 s methanol solution. As control, to prepare the devices with GO or PEDOT:PSS as hole transport layer, GO or PEDOT:PSS (~35 nm thick) were spin-coated onto ITO and then heated at 120°C for 30 min. The 36 mg/mL P3HT: $PC_{61}BM$ (1:0.8, w/w) blend was dissolved in *o*-dichlorobenzene by stirring at 50 °C overnight, which was spin-coated onto the hole transport layers at 800 rpm for 60 s, followed by annealing at 135 °C for 10 min in a nitrogen filled glove box. For the PBDTTT-C: $PC_{71}BM$ and PTB7: $PC_{71}BM$ devices, 25 mg/mL PBDTTT-C: $PC_{71}BM$ (1:1.5, w/w), 25 mg/mL PTB7: $PC_{71}BM$ (1:1.5, w/w) or 25 mg/mL PTB7-Th: $PC_{71}BM$ (1:1.5, w/w) blend dissolved in *o*-dichlorobenzene/1,8-diiodoctane (97:3 v/v) by stirring at room temperature overnight, which were spin-coated onto the hole transport layers at 1000 rpm for 60 s, respectively. Finally, Ca (10 nm) and Al (100 nm) were sequentially deposited atop of the active layer in a vacuum chamber with a pressure of about 4×10^{-5} Pa with a defined active area of $2 \times 5 \text{ mm}^2$.

For the SCLC measurements, hole-only devices were fabricated as follow: ITO was treated with UV light for 14 min, to prepare the device with P-GO as hole transport layer, 0.5 mg/mL aqueous GO was spin-coated onto ITO at 2000 rpm for 60 s and heated at 120°C for 30 min, followed by spin-coated 0.2 mg/mL P₂O₅ at 2000 rpm for 60 s methanol solution. As control, to prepare the devices with GO or PEDOT:PSS as hole transport layer, GO or PEDOT:PSS (~35 nm thick) were spin-coated onto ITO and then heated at 120°C for 30 min. The three active layers were spin-coated onto the HTLs, following by annealing at 135 °C for 10 min for P3HT:PC₆₁BM devices only. Finally, 50 nm Au was deposited atop the active layer in a vacuum chamber (~10⁻⁵Torr) with a defined active area of 2 × 5 mm².

Measurements and Characterization.

Atomic force microscopy (AFM) measurements were carried out on a Veeco DI-Multimode V scanning probe microscope in tapping mode. UV-Vis spectroscopy was recorded on a UV-vis-NIR 3600 spectrometer (Shimadzu, Japan). FTIR spectra were performed on a TENSOR 27 spectrometer (Bruker, Germany) at room temperature. The current density-voltage (J-V) characterization of inverted BHJ-PSC devices was carried out by using a Keithley 2400 source measurement unit under simulated AM 1.5 irradiation (100 mW·cm⁻²) with a standard Xenon-lamp-based solar simulator (SAN-EI ELECTRC CO., LTD 3A, Japan) solar simulator illumination intensity was calibrated by a monocrystalline silicon reference cell (AK-200) calibrated by the National Institute of Advanced Industrial Science and Technology (AIST). (SAN-EI ELECTRC CO., LTD 3A, Japan) solar simulator illumination intensity was calibrated by a monocrystalline silicon reference cell (AK-200) calibrated by the National Institute of Advanced Industrial Science and Technology (AIST). EQE spectra were measured in air using an ORIEL Intelligent Quantum Efficiency (IQE) 200™ Measurement system established with the tunable light source powered by a Xenon-lamp (150 W). All the measurements were carried out in air and a mask with well-defined area size of 10.0 mm² was attached onto the cell to define effective area so as to ensure accurate measurement. More than ten devices were fabricated and measured independently under each experimental condition to ensure the consistency of the data. The average PCE data were used in the discussions. Synchrotron radiation photoemission spectroscopy (SRPES) experiments were performed at the Catalysis and Surface Science endstation in the National Synchrotron Radiation Laboratory (NSRL), Hefei, and measured using synchrotron radiation light as the excitation source with a photon energy of 40 eV. A sample bias of -5 V was applied to observe the secondary electron cutoff.

S2. Mass spectrum of $(\text{CH}_3\text{O})_x\text{PO}(\text{OH})_{3-x}$.

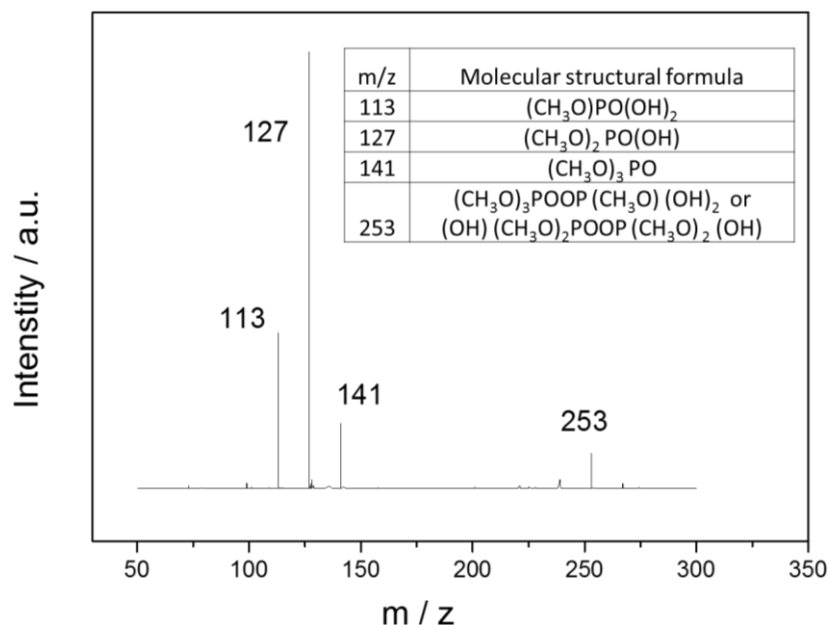


Figure S1. Mass spectrum of $(\text{CH}_3\text{O})_x\text{PO}(\text{OH})_{3-x}$ and the inset shows the possible molecular structural formula according to the m/z value.

S3. Effect of spin-coating speed of P_2O_5 solution on the performance of P-GO-based devices.

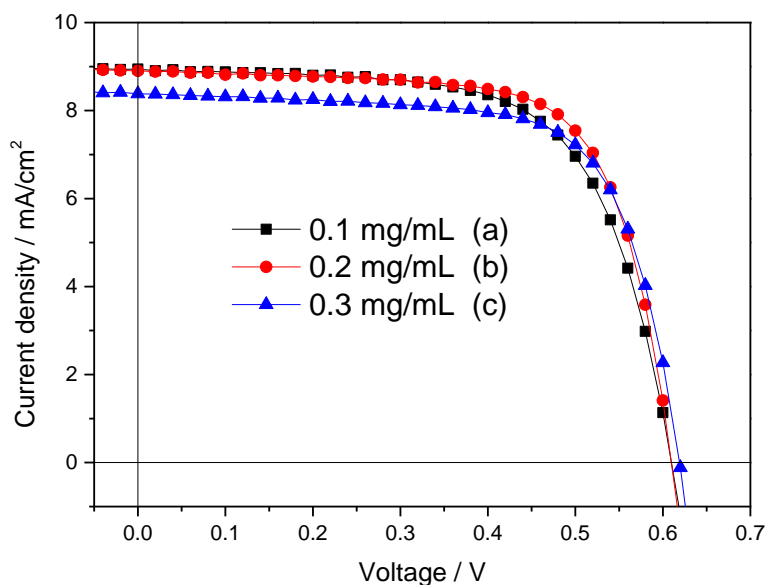


Figure S2. J-V Curves and Photovoltaic parameters of different concentrations of P_2O_5 in MeOH with a 2000 rpm on top of GO/ITO in the P3HT:PC₆₁BM-based devices.

Table S1. Photovoltaic parameters of the P3HT:PC₆₁BM-based devices based on P-GO HTL prepared from P₂O₅ precursor dissolved in MeOH with different initial concentrations.^a

| Concentration of P ₂ O ₅ (mg/mL) | V _{oc} (V) | J _{sc} (mA/cm ²) | FF (%) | PCE (%) |
|--|---------------------|---------------------------------------|--------|---------|
| 0.1 | 0.60 | 8.94 | 66.6 | 3.57 |
| 0.2 | 0.60 | 8.90 | 71.1 | 3.80 |
| 0.3 | 0.62 | 8.38 | 69.5 | 3.61 |

^a The spin-coating speed is fixed at 2000 rpm.

S4. Effect of the initial concentration of P₂O₅ dissolved in methanol solution on the performance of P-GO-based devices.

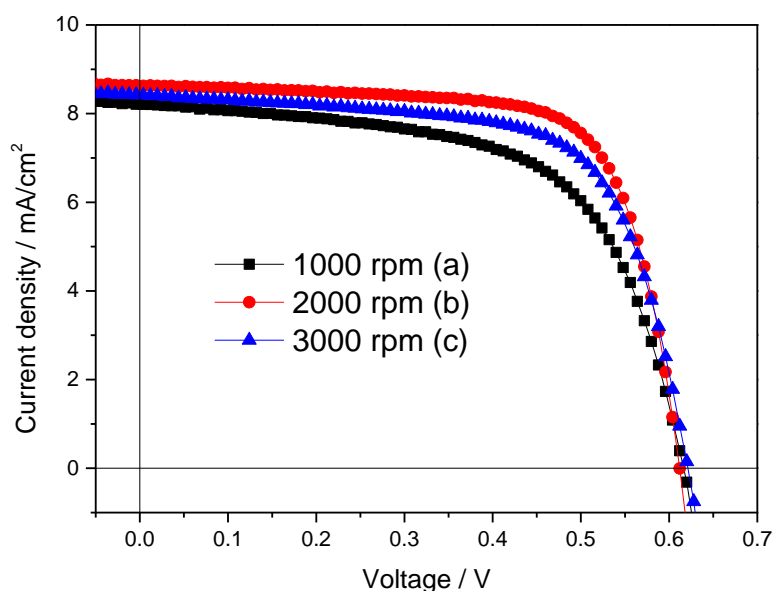


Figure S3. J-V Curves and Photovoltaic parameters of different rotational speed of P₂O₅ in MeOH with a 0.2 mg/mL concentration on top of GO/ITO in the P3HT:PC₆₁BM-based devices.

Table S2. Photovoltaic parameters of the P3HT:PC₆₁BM-based devices based on P-GO HTL prepared by spin-coating P₂O₅ precursor dissolved in MeOH onto GO layer with different spin-coating speed.^a

| Spin-coating speed | V _{oc} (V) | J _{sc} (mA/cm ²) | FF (%) | PCE (%) |
|--------------------|---------------------|---------------------------------------|--------|---------|
| 1000 rpm | 0.62 | 8.21 | 60.8 | 3.10 |
| 2000 rpm | 0.61 | 8.64 | 71.6 | 3.79 |
| 3000 rpm | 0.62 | 8.43 | 67.2 | 3.51 |

^a The concentration of P₂O₅ precursor dissolved in MeOH is fixed at 0.2 mg/ml.

S5. Effect of spin-coating speed of GO dispersion on the performance of GO-based devices.

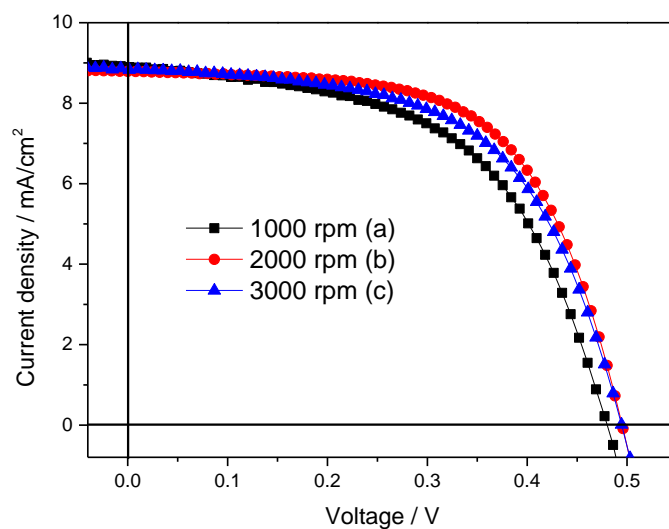


Figure S4. J-V Curves and Photovoltaic parameters of different rotational speed of GO aqueous solution on top of ITO in the P3HT:PC₆₁BM-based devices.

Table S3. Photovoltaic parameters of the P3HT:PC₆₁BM-based devices based on GO HTL prepared by spin-coating GO aqueous solution onto ITO with different spin-coating speed.

| Spin-coating speed | V _{oc} (V) | J _{sc} (mA/cm ²) | FF (%) | PCE (%) |
|--------------------|---------------------|---------------------------------------|--------|---------|
| 1000 rpm | 0.48 | 8.90 | 54.8 | 2.32 |
| 2000 rpm | 0.50 | 8.79 | 61.1 | 2.66 |
| 3000 rpm | 0.49 | 8.83 | 57.6 | 2.51 |

^a The concentration of GO aqueous dispersion is fixed at 0.5 mg/ml.

S6. Photovoltaic performance of P3HT:PC₆₁BM devices based on different HTLs.

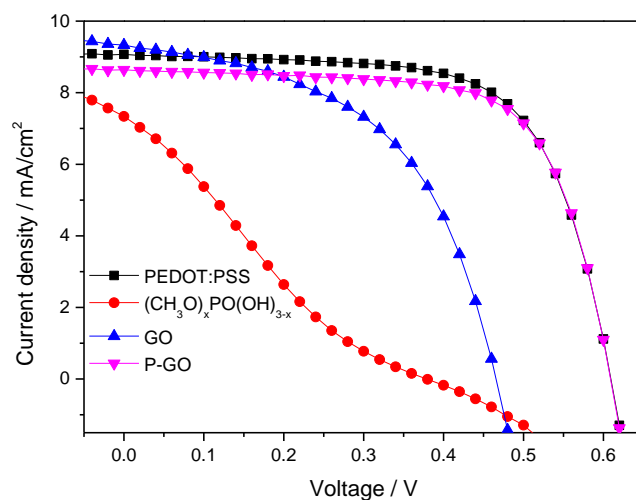


Figure S5. J-V Curves of P3HT:PC₆₁BM devices based on different HTLs.

Table S4. Photovoltaic parameters of P3HT:PC₆₁BM devices based on different HTLs.

| HTL | V _{oc} (V) | J _{sc} (mA/cm ²) | FF (%) | PCE (%) |
|--|---------------------|---------------------------------------|--------|---------|
| PEDOT:PSS | 0.60 | 9.07 | 67.80 | 3.69 |
| (CH ₃ O) _x PO(OH) _{3-x} | 0.38 | 7.34 | 21.53 | 0.60 |
| GO | 0.46 | 9.33 | 52.03 | 2.23 |
| P-GO | 0.60 | 8.64 | 69.87 | 3.62 |

S7. Transmittance spectra of ITO, ITO/PEDOT:PSS, ITO/GO and ITO/P-GO layers.

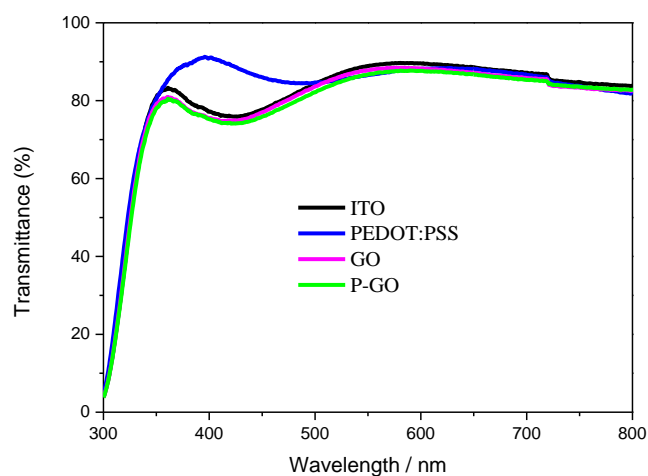


Figure S6. Transmittance spectra of ITO, ITO/PEDOT:PSS, ITO/GO and ITO/P-GO layers.

S8. Photovoltaic performance of the PTB7-Th:PC₇₁BM devices based on different HTLs.

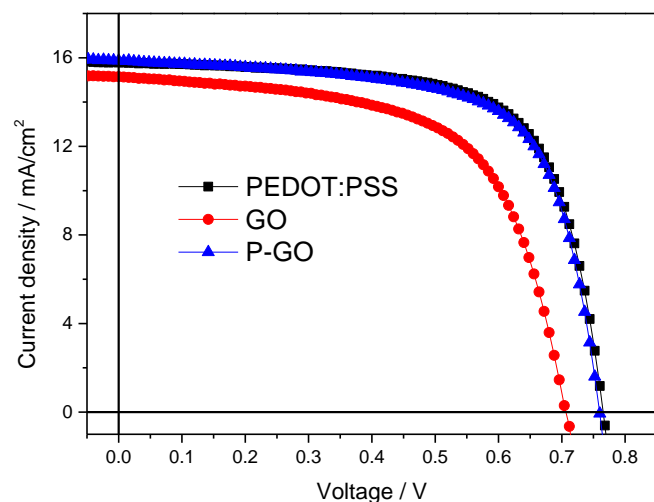


Figure S7. J-V curves of PTB7-Th:PC₇₁BM devices based on different HTLs.

Table S5. Photovoltaic parameters of the PTB7-Th:PC₇₁BM devices based on different HTLs.

| HTL | V _{oc} (V) | J _{sc} (mA/cm ²) | FF (%) | PCE (%) |
|-----------|---------------------|---------------------------------------|--------|---------|
| PEDOT:PSS | 0.77 | 15.79 | 68.36 | 8.29 |
| GO | 0.70 | 15.15 | 61.69 | 6.58 |
| P-GO | 0.76 | 15.87 | 67.77 | 8.18 |

According to the comparison of PTB7-Th:PC₇₁BM devices based on different HTLs as shown in Figure S7 and Table S5, when using P-GO HTL, the PCE of the device reaches 8.18% calculated from a V_{oc} of 0.76 V, a J_{sc} of 15.87 mA/cm² and a FF of 67.77%. Such a PCE of 8.18% is improved by ~24.3% relative to that of device based on pristine GO HTL with a PCE of 6.58%, and close to that of PEDOT:PSS-based device with a PCE of 8.29% (a V_{oc} of 0.77 V, a J_{sc} of 15.79 mA/cm² and a FF of 68.36%), indicating the P-GO can also be used as a substitute to PEDOT:PSS HTL in a popular active layer system of PTB7-Th:PC₇₁BM.

S9. Enhancement ratios of the photovoltaic parameters.

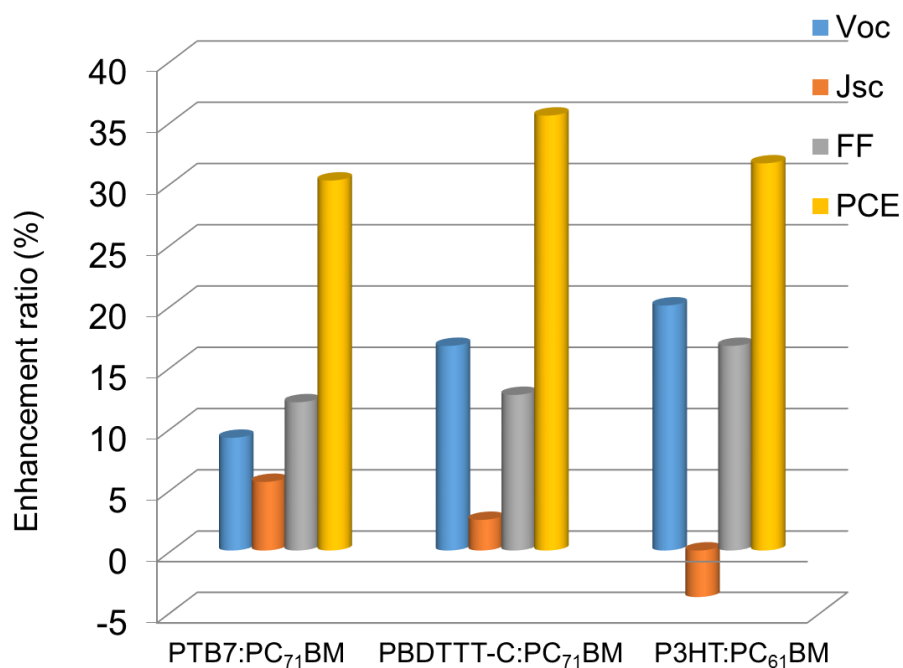


Figure S8. Enhancement ratios of the photovoltaic parameters (V_{oc}, J_{sc}, FF, and PCE) of P-GO-based devices compared to those of GO-based devices.

S10. Contact angles of water droplet on bare ITO, PEDOT:PSS, GO, and P-GO.

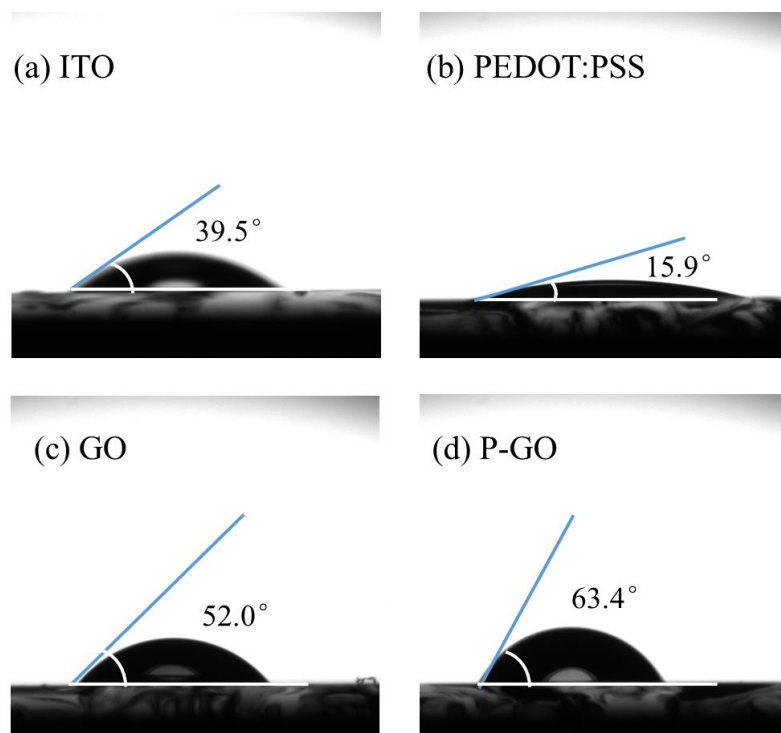


Figure S9. Contact angles of water droplet on bare ITO (a), PEDOT:PSS (b), GO (c), and P-GO (c).

S11. Work functions of ITO, PEDOT:PSS, GO, and P-GO.

Table S6. The secondary electron thresholds and work functions of ITO, ITO/PEDOT:PSS, ITO/GO, and ITO/P-GO.

| Sample | Secondary Electron Threshold ^b (E_{th} , eV) | Work Function ^b (Φ , eV) |
|-----------------------|---|--|
| ITO | 35.36 | 4.64 |
| ITO/PEDOT:PSS | 35.18 | 4.82 |
| ITO/GO | 35.76 | 4.24 |
| ITO/P-GO ^a | 35.30 | 4.70 |

^a The solution of P_2O_5 dissolved in methanol (0.2 mg/mL) was spin-coated on the top of GO film with a 2000 rpm.

^b The work function (Φ) is determined from the secondary electron threshold as $\Phi = h\nu - E_{th}$, where $h\nu$ and E_{th} are the photon energy of excitation light (synchrotron radiation light, 40 eV) and the secondary electron threshold energy, respectively.

S12. High-resolution P2p XPS spectra of $(CH_3O)_xPO(OH)_{3-x}$ and $(CH_3O)_xPO(OH)_{3-x}/GO$.

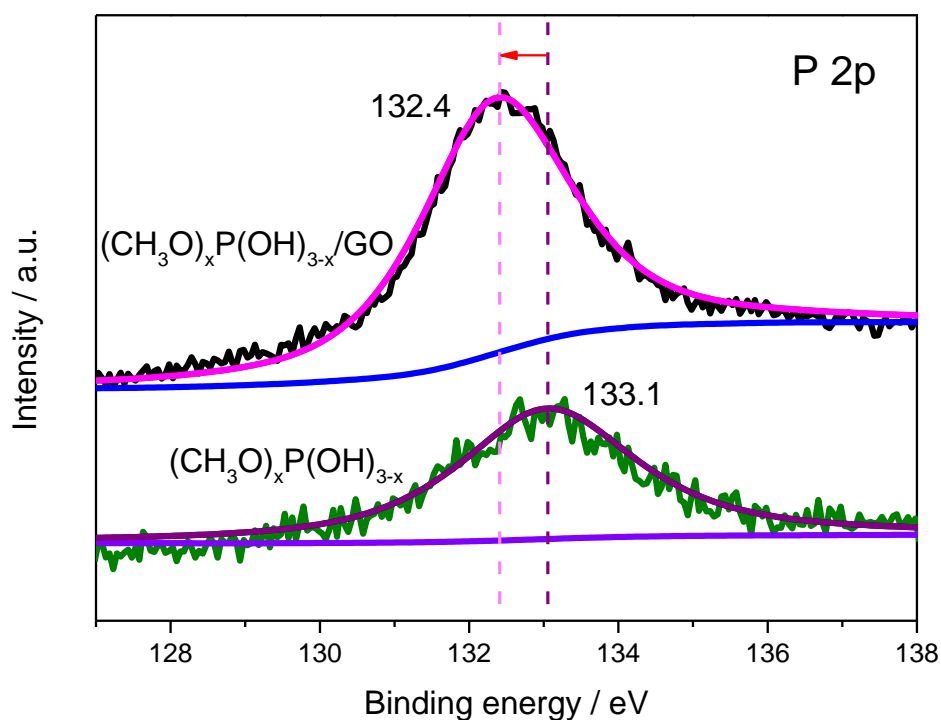


Figure S10. Deconvoluted high-resolution P2p XPS spectra of $(CH_3O)_xPO(OH)_{3-x}$ and $(CH_3O)_xPO(OH)_{3-x}/GO$.

S13. Raman spectra of GO and P-GO.

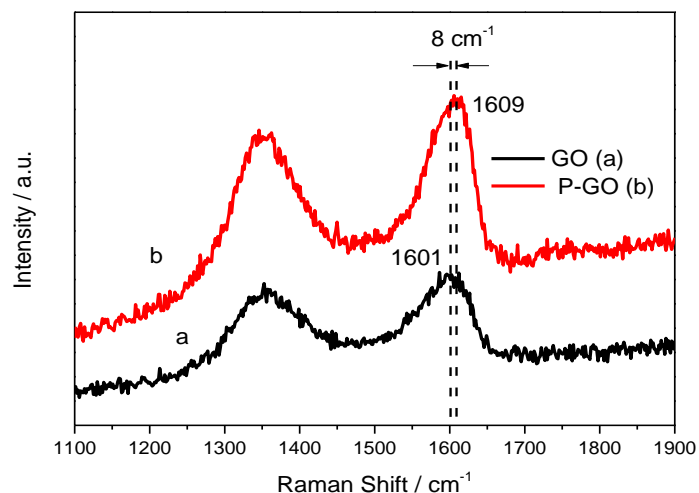


Figure S11. Raman spectra of GO (a) and P-GO (b).

In previous reports, the down-shifting of the G band of GO was interpreted by electron accepting^{S1}, while the up-shifting of the G band was due to electron donating of GO^{S2}. Herein, after spin-coating the solution of P₂O₅ dissolved in methanol, we found that the G band of GO up-shifted by 8 cm⁻¹ from 1601 to 1609 cm⁻¹, suggesting the electron transfer from GO to (CH₃O)_xPO(OH)_{3-x}.

S14. Hole mobility of the devices with different HTLs.

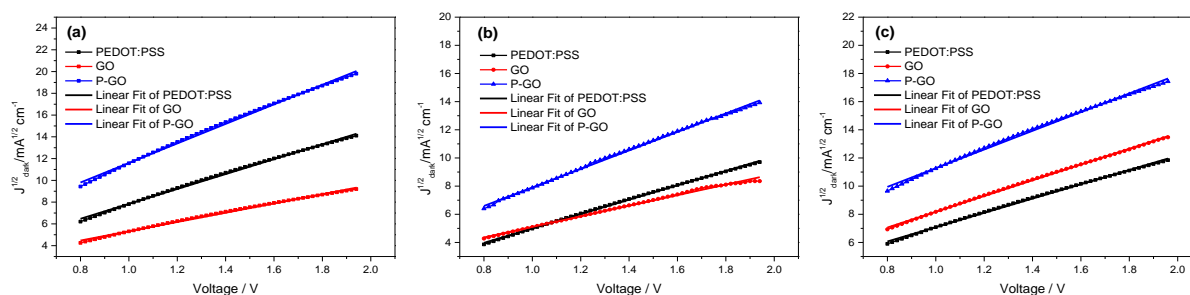


Figure S12. $J^{1/2}$ -V (derived from Fig. 5 of main text) and the corresponding fitting curves of the hole-only ITO/HTL/active layer/MoO₃/Ag devices based on different active layer systems and HTLs. (a) PTB7:PC₇₁BM, (b) PBDTTT-C:PC₇₁BM, (c) P3HT:PC₆₁BM.

Table S7. Hole mobilities of the devices based on PEDOT:PSS, GO, and P-GO HTLs.

| Active layer | HTL | μ_h (cm ² V ⁻¹ s ⁻¹) |
|------------------------------|-----------|--|
| PTB7:PC ₇₁ BM | PEDOT:PSS | 1.32×10 ⁻⁴ |
| | GO | 5.05×10 ⁻⁵ |
| | P-GO | 2.27×10 ⁻⁴ |
| PBDTTT-C:PC ₇₁ BM | PEDOT:PSS | 7.41×10 ⁻⁵ |
| | GO | 3.85×10 ⁻⁵ |
| | P-GO | 1.23×10 ⁻⁴ |
| P3HT:PC ₆₁ BM | PEDOT:PSS | 3.62×10 ⁻⁴ |
| | GO | 4.41×10 ⁻⁴ |
| | P-GO | 6.18×10 ⁻⁴ |

Supplementary references

- S1. S. X. Qu, M. H. Li, L. X. Xie, X. Huang, J. G. Yang, N. Wang and S. F. Yang, *ACS Nano*, 2013, **7**, 4070.
- S2. E. S. Choi, Y. J. Jeon, S. S. Kim, T. W. Kim, Y. J. Noh, S. N. Kwon and S. I. Na, *Appl. Phys. Lett.*, 2015, **107**, 023301.